

Including heavy quark production in PDF fits HERA - LHC Workshop 2007

Amanda Cooper-Sarkar
Oxford University

Abstract

At HERA heavy quarks may contribute up to 30% of the structure function F_2 . The introduction of heavy quarks requires an extension of the DGLAP formalism. The effect of using different heavy flavour number schemes, and different approaches to the running of α_s , are compared using the ZEUS PDF fit formalism. The potential of including charm data in the fit is explored, using D^* double differential cross-sections rather than the inclusive quantity $F_2^{c\bar{c}}$.

Parton Density Function (PDF) determinations are usually global fits [1–4], which use inclusive cross-section data and structure function measurements from deep inelastic lepton hadron scattering (DIS) data as well as some other exclusive cross-sections. The kinematics of lepton hadron scattering is described in terms of the variables Q^2 , the invariant mass of the exchanged vector boson, Bjorken x , the fraction of the momentum of the incoming nucleon taken by the struck quark (in the quark-parton model), and y which measures the energy transfer between the lepton and hadron systems. The differential cross-section for the neutral current (NC) process is given in terms of the structure functions by

$$\frac{d^2\sigma(e^\pm p)}{dx dQ^2} = \frac{2\pi\alpha^2}{Q^4 x} \left[Y_+ F_2(x, Q^2) - y^2 F_L(x, Q^2) \mp Y_- x F_3(x, Q^2) \right],$$

where $Y_\pm = 1 \pm (1 - y)^2$. In the HERA kinematic range there is a sizeable contribution to the F_2 structure function from heavy quarks, particularly charm. Thus heavy quarks must be properly treated in the formalism. Furthermore fitting data on charm production may help to give constraints on the gluon PDF at low- x .

The most frequent approaches to the inclusion of heavy quarks within the conventional framework of QCD evolution using the DGLAP equations [5–8] are ¹:

- ZM-VFN (zero-mass variable flavour number schemes) in which the charm parton density $c(x, Q^2)$ satisfies $c(x, Q^2) = 0$ for $Q^2 \leq \mu_c^2$ and $n_f = 3 + \theta(Q^2 - \mu_c^2)$ in the splitting functions and β function. The threshold μ_c^2 , which is in the range $m_c^2 < \mu_c^2 < 4m_c^2$, is chosen so that $F_2^c(x, Q^2) = 2e_c^2 x c(x, Q^2)$ gives a satisfactory description of the data. The advantage of this approach is that the simplicity of the massless DGLAP equations is retained. The disadvantage is that the physical threshold $\hat{W}^2 = Q^2(\frac{1}{z} - 1) \geq 4m_c^2$ is not treated correctly (\hat{W} is the γ^*g CM energy).
- FFN (fixed flavour number schemes) in which there is no charm parton density and all charmed quarks are generated by the BGF process. The advantage of the FFNS scheme is that the threshold region is correctly handled, but the disadvantage is that large $\ln(Q^2/m_c^2)$ terms appear and charm has to be treated ab initio in each hard process.
- GM-VFN (general mass variable flavour number schemes), which aim to treat the threshold correctly and absorb $\ln(Q^2/m_c^2)$ terms into a charm parton density at large Q^2 . There are differing versions of such schemes [9, 10]

For the main ZEUS-S analysis [4], the heavy quark production scheme used was the general mass variable flavour number scheme of Roberts and Thorne (TR-VFN) [10, 11]. However we also investigated the use of the FFN for 3-flavours and the ZM-VFN. In Fig. 1 we compare the fit prediction

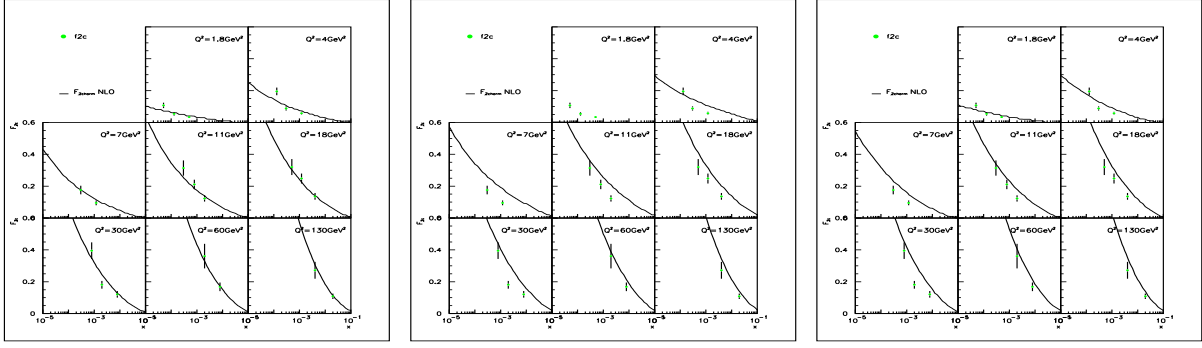


Fig. 1: ZEUS data on $F_2^{c\bar{c}}$ compared to predictions using the FFN (left) ZM-VFN (middle), TR-VFN (right) schemes. In each case the fit parameters are kept the same (fitted using FFN) and only the scheme is changed.

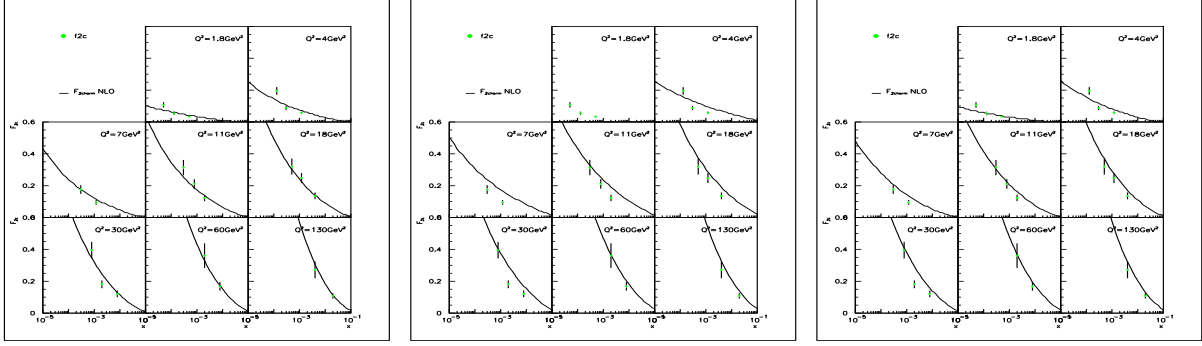


Fig. 2: ZEUS data on $F_2^{c\bar{c}}$ compared to predictions using the FFN (left) ZM-VFN (middle), TR-VFN (right) schemes. In each case the fit parameters are refitted when the scheme is changed.

for $F_2^{c\bar{c}}$ using each of these schemes to data on $F_2^{c\bar{c}}$ from the ZEUS collaboration [12]. One can see the differences between the FFN and the ZM-VFN at threshold where the ZM-VFN is clearly inadequate. In this kinematic region the TR-VFN is more like the FFN. However, the TR-VFN scheme becomes more like the ZM-VFN scheme for $Q^2 \gg m_c^2$.

This comparison illustrates the effect of change in scheme when keeping the PDF parameters fixed. In practice one should refit the PDF parameters using the alternative schemes. The result of this is shown in Fig 2. The difference between the FFN and TR-VFN is not so marked. It is well known that these choices have some effect on the steepness of the gluon at very small- x , such that the zero-mass choice produces a slightly less steep gluon. In Fig 3 the differing shapes of the sea and the gluon PDFs for these different heavy quark schemes are illustrated.

Figure 4 shows the ZEUS-S fit predictions for more recent $F_2^{c\bar{c}}$ data from ZEUS and H1 [13, 14].

¹Charm production is described here but a similar formalism describes beauty production

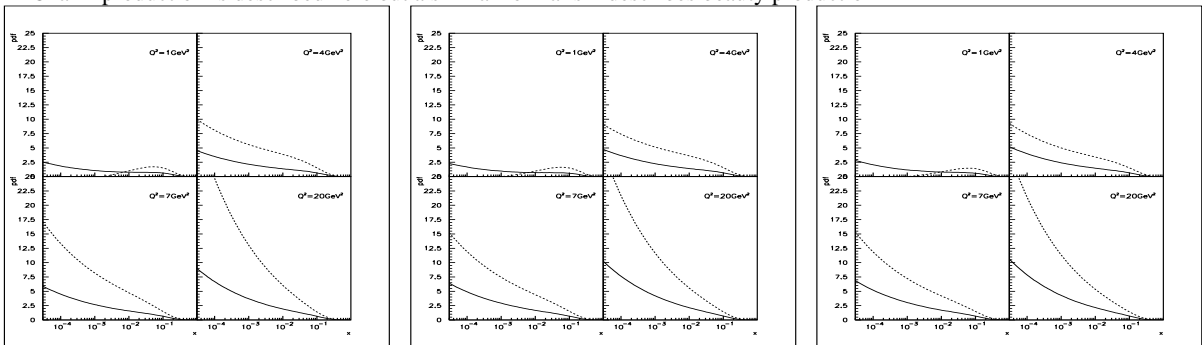


Fig. 3: The sea and gluon PDFs extracted from fits using the FFN (left) ZM-VFN (middle), TR-VFN (right) schemes. In each case the fit parameters are refitted when the scheme is changed

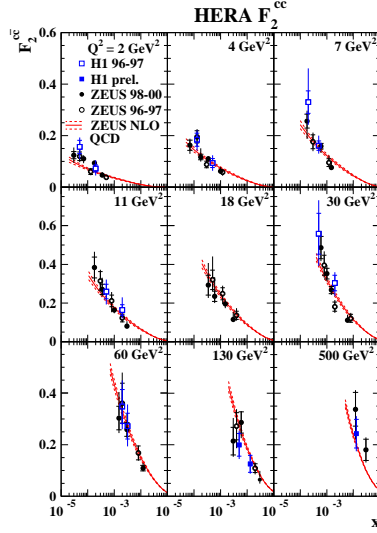


Fig. 4: Comparison of ZEUS PDF fit predictions to recent charm data from ZEUS and H1 on $F_2^{c\bar{c}}$

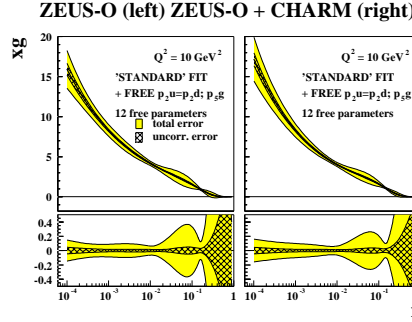


Fig. 5: The gluon PDF and its fractional uncertainties at $Q^2 = 10\text{GeV}^2$, from a) the ZEUS-O PDF fit (left) and b) a similar fit with $F_2^{c\bar{c}}$ data included (right).

The scheme chosen was FFN for 3 flavours with the renormalisation and factorisation scale for light quarks both set to Q^2 but the factorisation scale for heavy quarks set to $Q^2 + 4m_c^2$. The reason for these choices of scheme and scale is that these are the choices made in the programme HVQDIS [15–17] which was used to extract $F_2^{c\bar{c}}$ from data on D^* production. The scale choice does not make any significant difference to the predictions (see later).

Note that in Fig 4 the charm data are shown compared to the ZEUS-S PDF fit predictions but these data were not input to the fit. Including the ZEUS charm data [13] in the ZEUS-S PDF fit gives no visible improvement to PDF uncertainties. To investigate the potential of charm data to constrain the gluon PDF, we modified the ZEUS-S PDF fit as follows: all ZEUS inclusive neutral current and charged current cross-section data from HERA-I was included but no fixed target data; the parametrisation was modified to free the mid- x gluon parameter $p_5(g)$ and the low- x valence parameter $p_2(u) = p_2(d)$, however the $\bar{d} - \bar{u}$ normalisation had to be fixed since there is no information on this without fixed target data. This fit is called the ZEUS-O fit. Fig. 5 compares the gluon PDF and its uncertainties as extracted from this ZEUS-O PDF fit with the those extracted from a similar fit including the $F_2^{c\bar{c}}$ data. This illustrates that the charm data has the potential to constrain the gluon PDF uncertainties. Its lack of impact on the global fit may be because we are not using the charm data optimally.

$F_2^{c\bar{c}}$ is a quantity extracted from D^* cross-sections by quite a large extrapolation. It would be better to fit to those cross-sections directly. The evaluation of the theoretical predictions involves running the NLO programme HVQDIS for each iteration of the fit. However, one can shorten this process by using the same method as was used for the ZEUS-JETS fit [18]. The PDF independent subprocess cross-

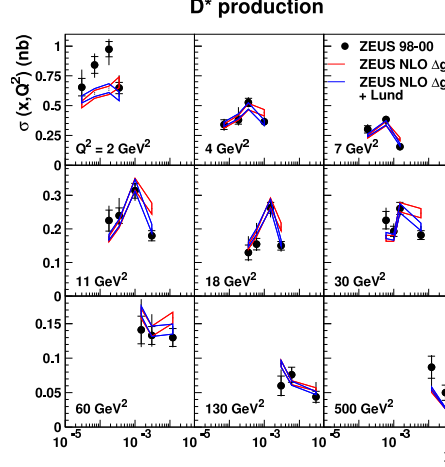


Fig. 6: Double differential cross-sections for D^* production. The red lines show the predictions of the ZEUS-S-13 NLO PDF fit using the Petersen fragmentation function for the D^* , whereas the blue lines show these predictions using the Lund fragmentation function.

sections are output onto a grid, such that they can simply be multiplied by the PDFs at each iteration. The data used are the nine double differential cross-section measurements of $d^2\sigma(D^*)/dQ^2 dy$ [13], see Fig. 6

There are further theoretical considerations to be accounted for when unputting D^* cross-sections, as opposed to an inclusive quantity like F_2^{cc} , to a PDF fit. Since the grids are calculated using HVQDIS the fit must use the FFN scheme to be compatible. This means that we cannot use ZEUS high- Q^2 data, since this scheme is not suitable at high- Q^2 . Hence we chose to use the ZEUS-S global fit, which included fixed target data, with a cut-off $Q^2 < 3000 \text{ GeV}^2$. Furthermore, it has only recently become evident that since we are using the FFN scheme we must also treat the running of α_s differently than in the VFN schemes. In these VFN schemes α_s is matched at flavour thresholds [19], but the slope of α_s is discontinuous at the flavour thresholds. For consistency with HVQDIS we must use a 3-flavour α_s which is continuous in Q^2 . This requires an equivalent value of $\alpha_s(M_Z) = 0.105$ in order to be consistent, at low Q^2 , with the results of using a value of $\alpha_s(M_Z) = 0.118$ in the usual VFN schemes. Such a 3-flavour α_s has also been used in specialised PDF fits of MRST (MRST2004F3) [20], which are used to make predictions for charm production.

In Fig 7 we compare different heavy quark factorisation scales and different treatments of the running of α_s for predictions of F_2^{cc} . Fig. 8 makes the same comparison for F_2^{bb} ². We see that within the FFN scheme the choice of the heavy quark factorisation scale makes only a small difference at low Q^2 . The treatment of α_s gives larger differences. The FFN scheme and TR-VFN scheme differ for almost all Q^2 if α_s runs as for the VFN schemes. However if a 3-flavour α_s is applied in the FFN schemes there is much better agreement of all schemes at higher Q^2 .

We now return to consider inputting the D^* cross-sections to the PDF fit. The ZEUS-S global fit formalism is used including all ZEUS inclusive neutral and charged current cross-section data from HERA-I and the fixed target data. The parametrisation was also modified to free the mid- x gluon parameter $p_5(g)$ and the low- x valence parameter $p_2(u) = p_2(d)$. This fit is called ZEUS-S-13. Figure 9 shows the difference in the gluon PDF uncertainties, before and after the D^* cross-sections were input to the ZEUS-S-13 global fit. Disappointingly the uncertainty on the gluon is NOT much improved.

Should we have expected much improvement? There are two aspects of the fit which could be improved. The predictions for the D^* cross-sections have more uncertainties than just the PDF parametrization. A further uncertainty is introduced in the choice of the $c \rightarrow D^*$ fragmentation. The Petersen frag-

²Note the predictions are always made by refitting PDF parameters for each scheme choice, not by simply changing the scheme with the same PDF parameters

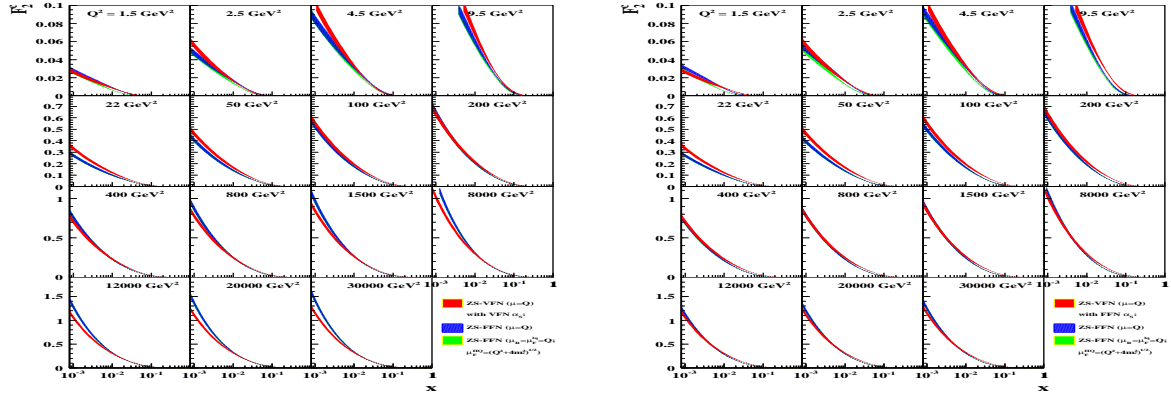


Fig. 7: Comparison of predictions for $F_2^{c\bar{c}}$, from fits which use the TR-VFN scheme and the FFN scheme with two different

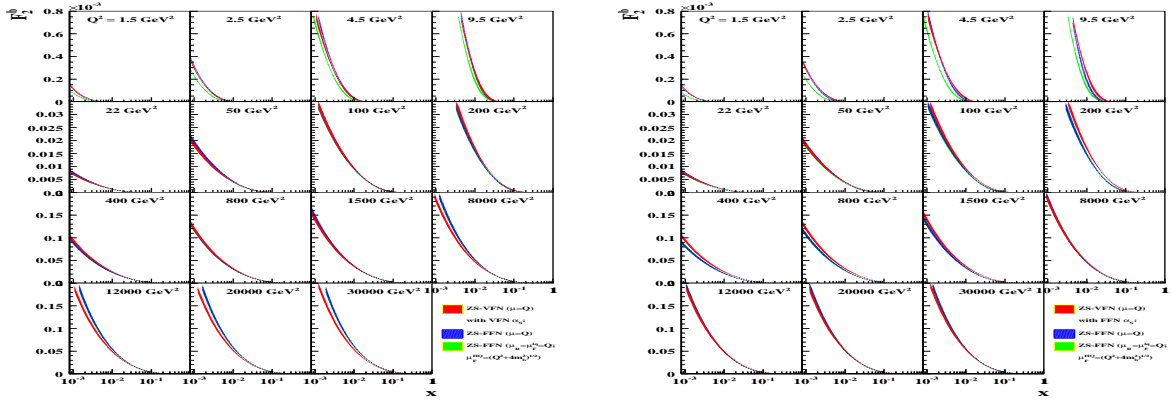


Fig. 8: Comparison of predictions for $F_2^{b\bar{b}}$, from fits which use the TR-VFN scheme and the FFN scheme with two different factorisation scales: on the left hand side the FFN schemes still use a VFN treatment of α_s , whereas on the right hand side a 3-flavour α_s is used.

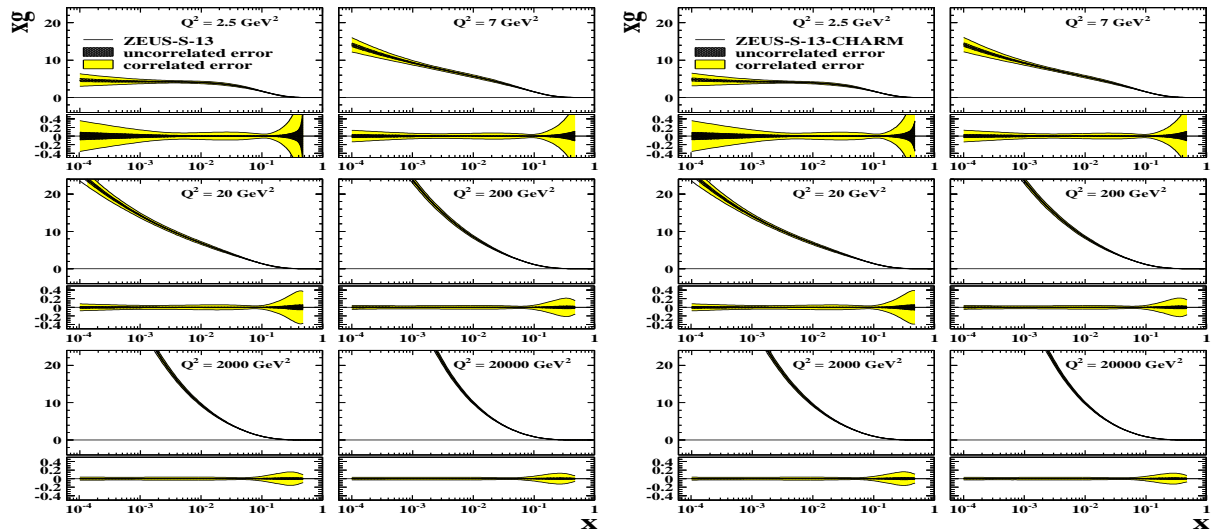


Fig. 9: The gluon PDF and its fractional uncertainties for various Q^2 bins Left: before D^* cross-section data are input to the ZEUS-S-13 fit. Right: after D^* cross-section data are input to the ZEUS-S-13 fit

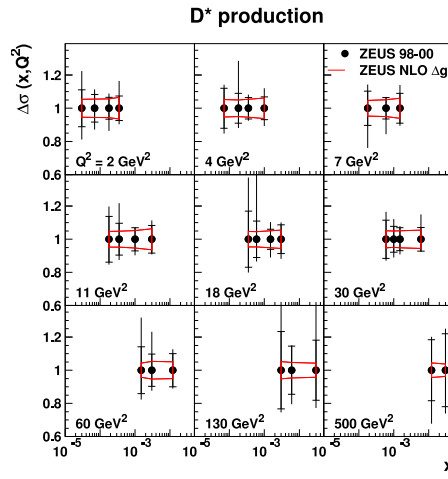


Fig. 10: Fractional uncertainties on double differential cross-sections for D^* production. the red lines show the uncertainties on these cross-sections deriving from the uncertainty on the gluon PDF in the ZEUS-S-13 fit, before including these D^* data in the fit.

mentation function was used for the fit predictions. However, looking back at Fig 6 we can see that the Lund fragmentation function seems to describe the data better. To best exploit the charm data in future we need to address such aspects of our model uncertainty. Secondly, Fig 10 compares the fractional errors on the D^* cross-sections with the uncertainty on the prediction for these quantities derived from the uncertainty on the gluon PDF in the ZEUS-S-13 PDF fit, before inputting the D^* cross-sections. The data errors are larger than the present level of uncertainty. Thus we eagerly await the 5-fold increase in statistics expected from HERA-II charm and beauty data.

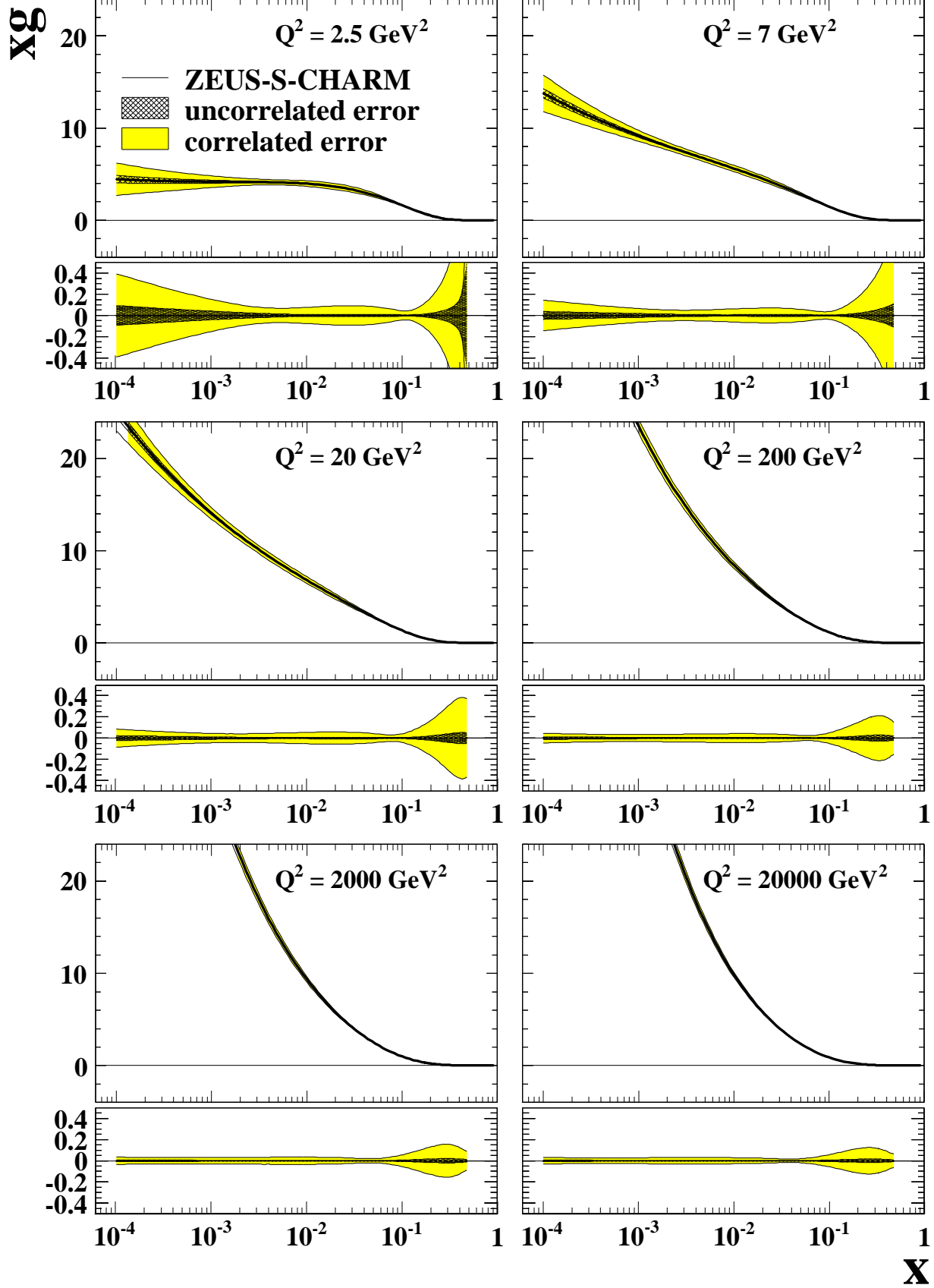
1 Acknowledgements

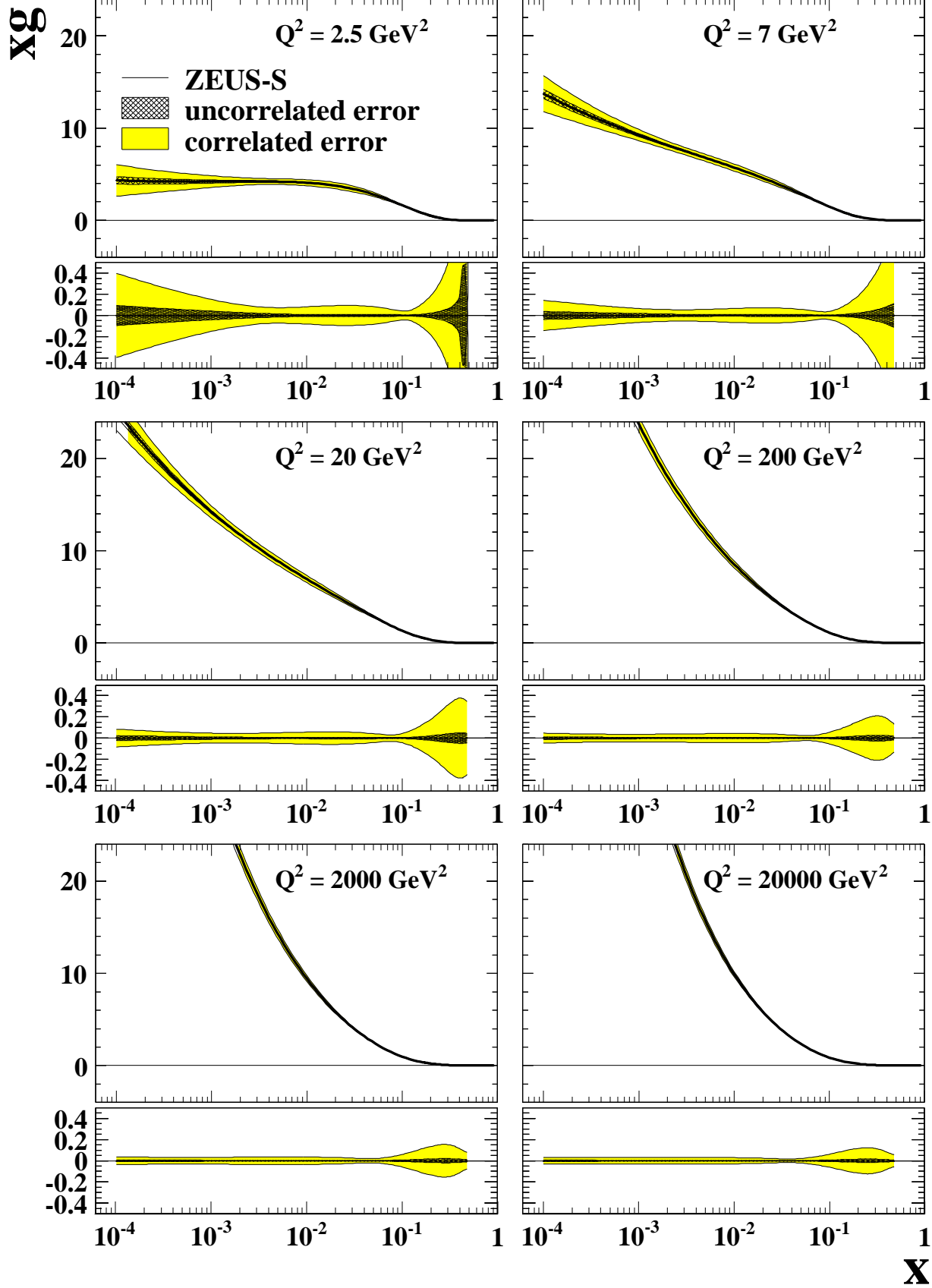
I would like to thank members of the ZEUS collaboration who have worked on the inclusion of heavy flavour data in the PDF fits, particularly: C Gwenlan, E Tassi, J Terron, M Wing, M Botje. I thank R Thorne and P thompson for useful discussions.

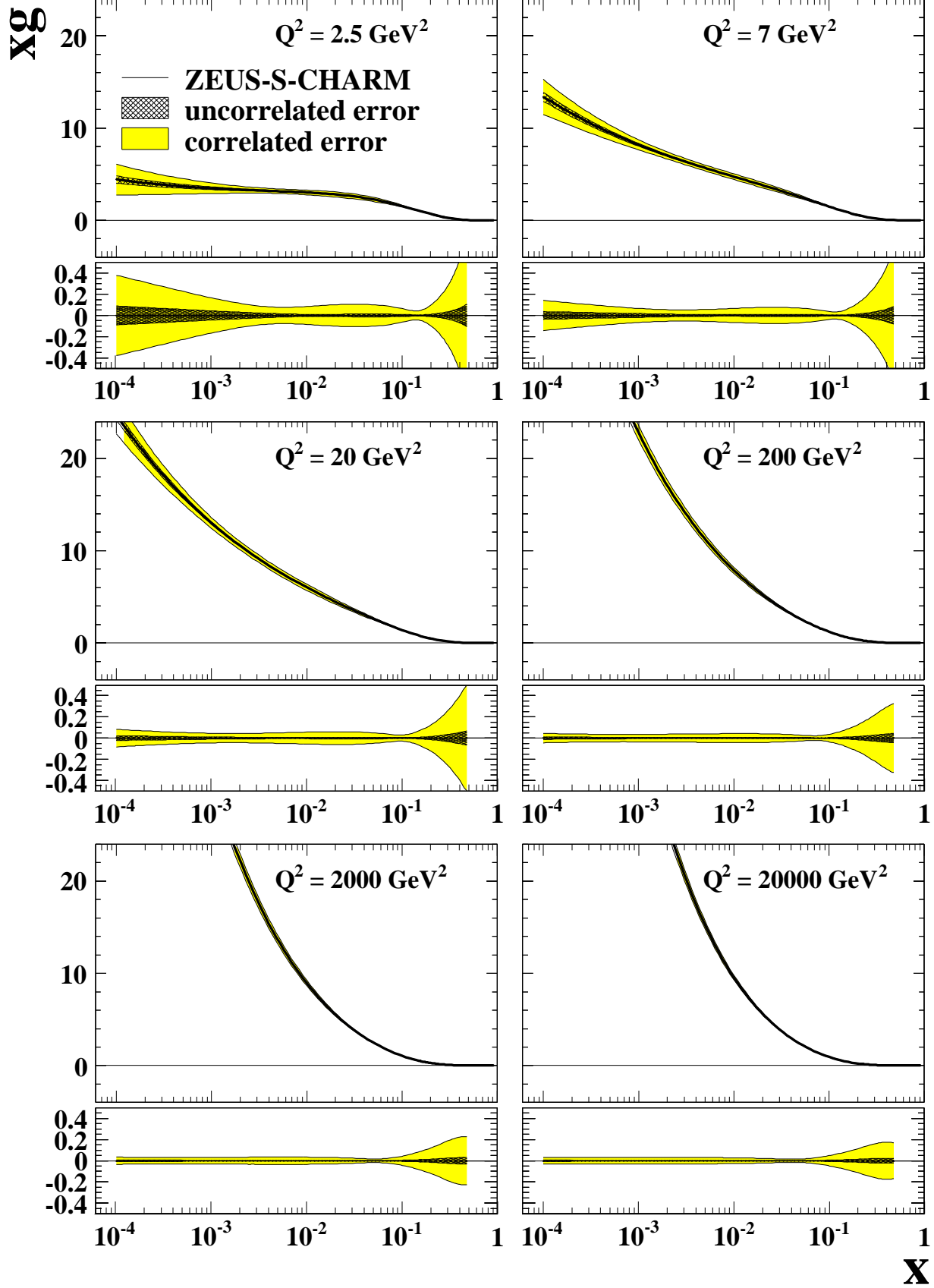
References

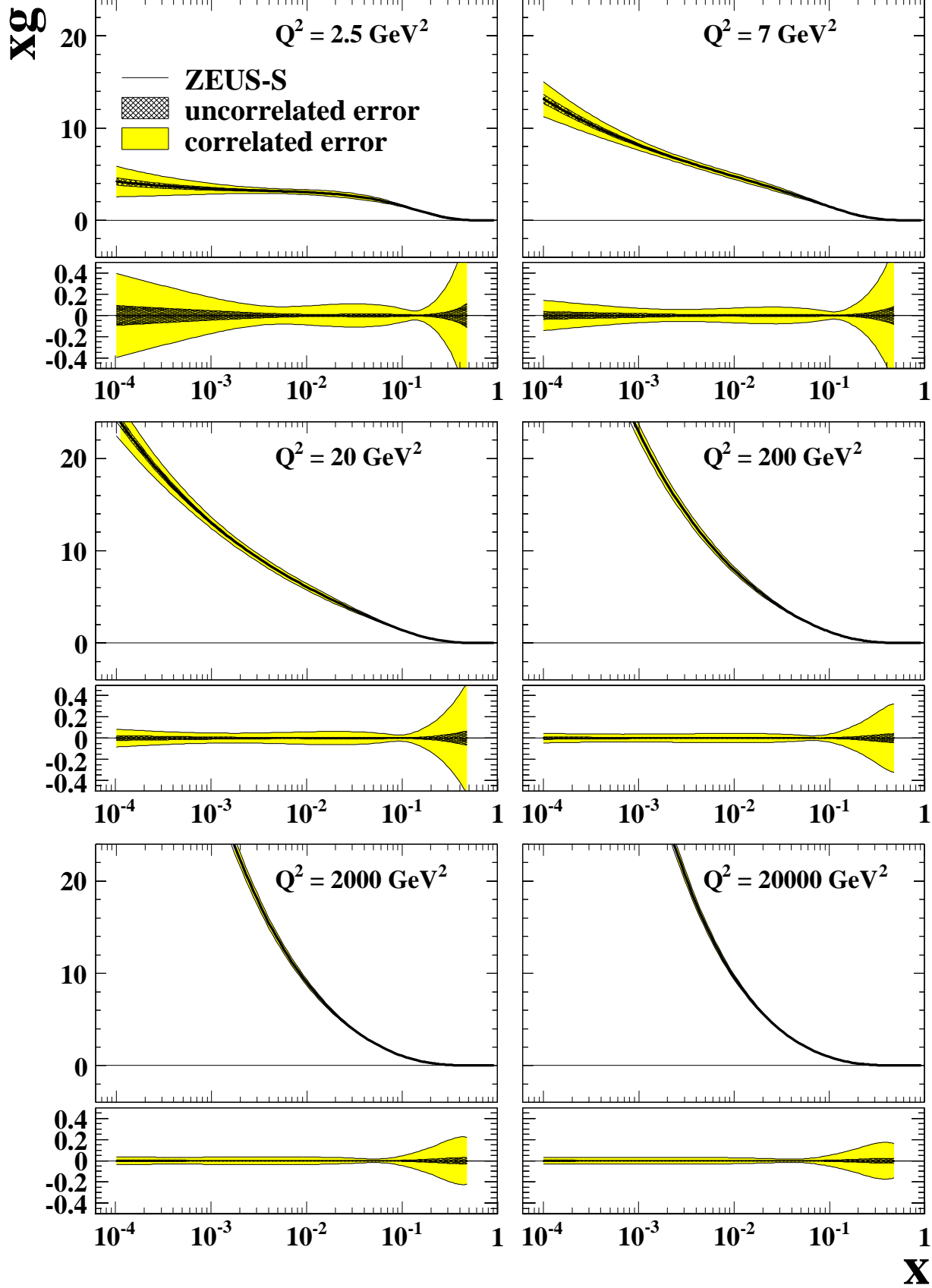
- [1] A.D. Martin et al., Eur. Phys.J **C23**, 73 (2002).
- [2] A.D. Martin et al., arxiv **0706**, 0459 (2007).
- [3] J. Pumplin et al., JHEP **0207**, 012 (2002).
- [4] ZEUS Coll., S. Chekanov et al., Phys. Rev **D 67**, 012007 (2003).
- [5] G. Altarelli, G. Parisi, Nucl.Phys. **B126**, 298 (1977).
- [6] V.N. Gribov, L.N. Lipatov, Sov.J.Nucl.Phys **15**, 438 (1972).
- [7] L.N. Lipatov, Sov.J.Nucl.Phys **20**, 94 (1975).
- [8] Yu.L. Dokshitzer, JETP **46**, 641 (1977).
- [9] Wu Ki Tung et al., JHEP **0702**, 053 (2007).
- [10] R.S. Thorne, Phys.Rev **D73**, 054019 (2006).
- [11] R.S. Thorne and R.G. Roberts, Phys.Rev **D57**, 6871 (1998).
- [12] ZEUS Coll., S. Chekanov et al., Eur.Phys.J **C 12**, 1 (2000).
- [13] ZEUS Coll., S. Chekanov et al., Phys. Rev **D 69**, 012004 (2004).

- [14] H1 Coll., C.Adloff et al., Eur.Phys.J **C 40**, 349 (2005).
- [15] B.W. Harris and J. Smith, N.Phys **B 452**, 109 (1995).
- [16] B.W. Harris and J. Smith, Phys.Lett. **B 353**, 535 (1995).
- [17] B.W. Harris and J. Smith, Phys.Lett. **B 359**, 423 (1995).
- [18] ZEUS Coll., S. Chekanov et al., Eur.Phys.J **C 42**, 1 (2005).
- [19] W.J. Marciano, Phys.Rev. **D 29**, 5801 (1984).
- [20] A.D. Martin et al., Phys. Lett. **B636**, 259 (2006).

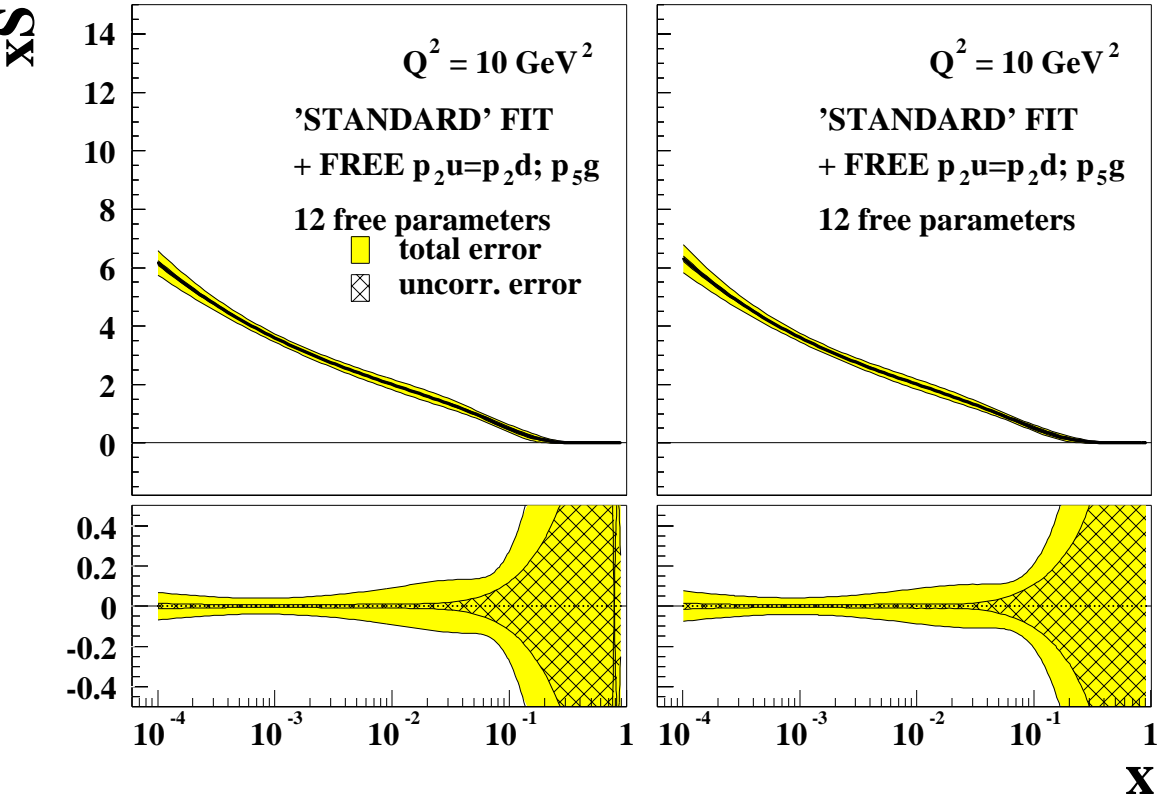




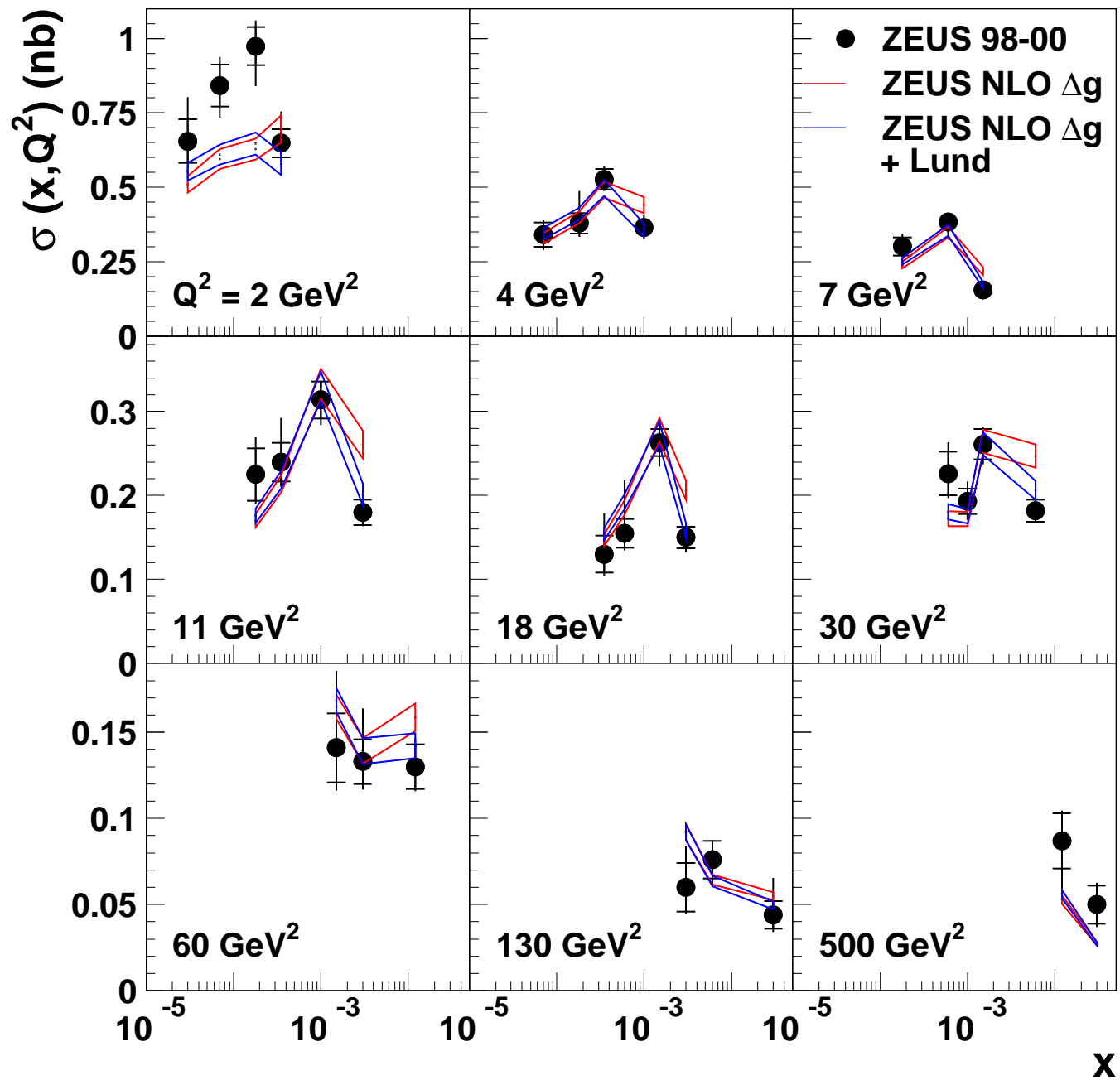




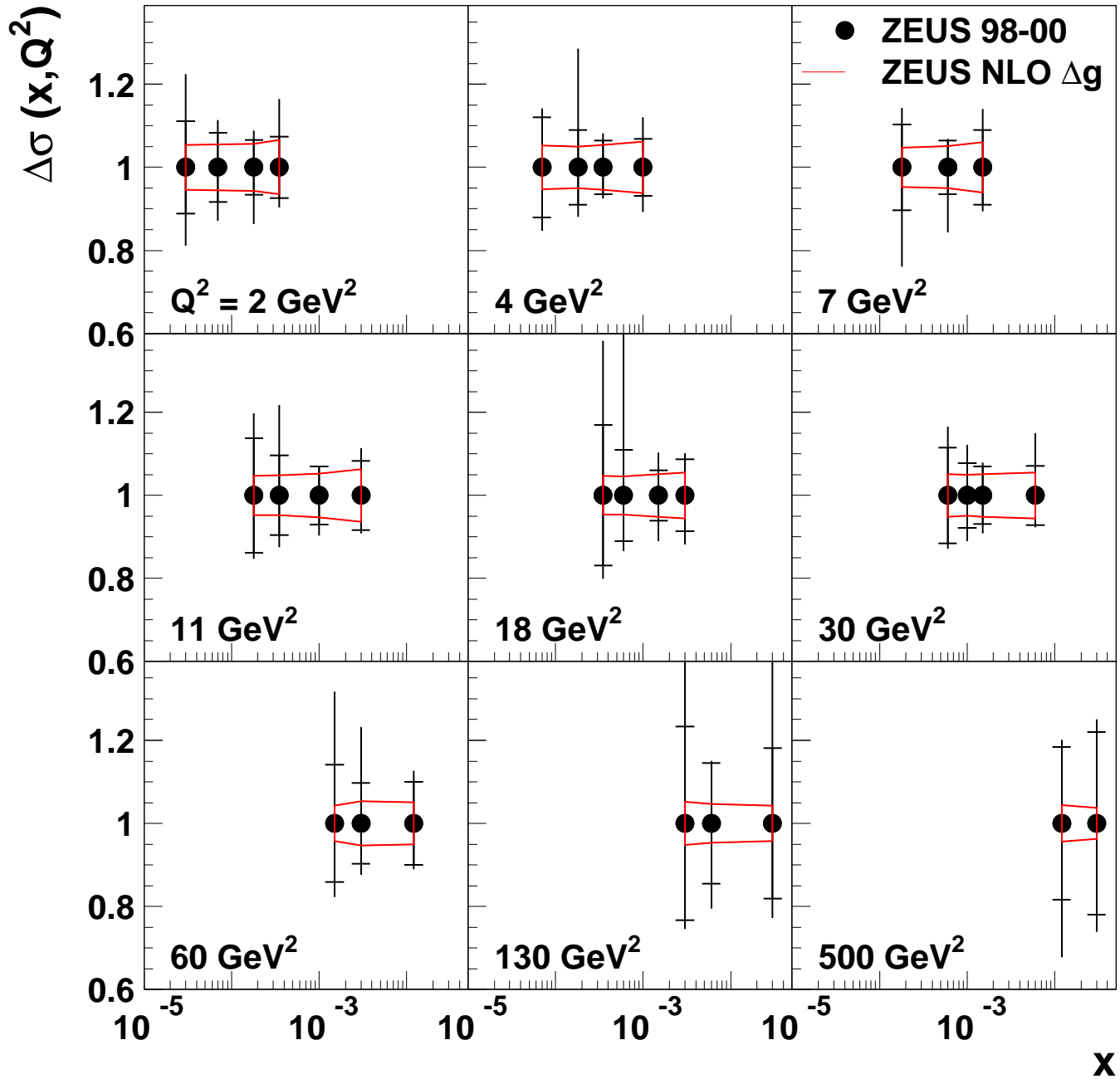
ZEUS-O (left) ZEUS-O + CHARM (right)



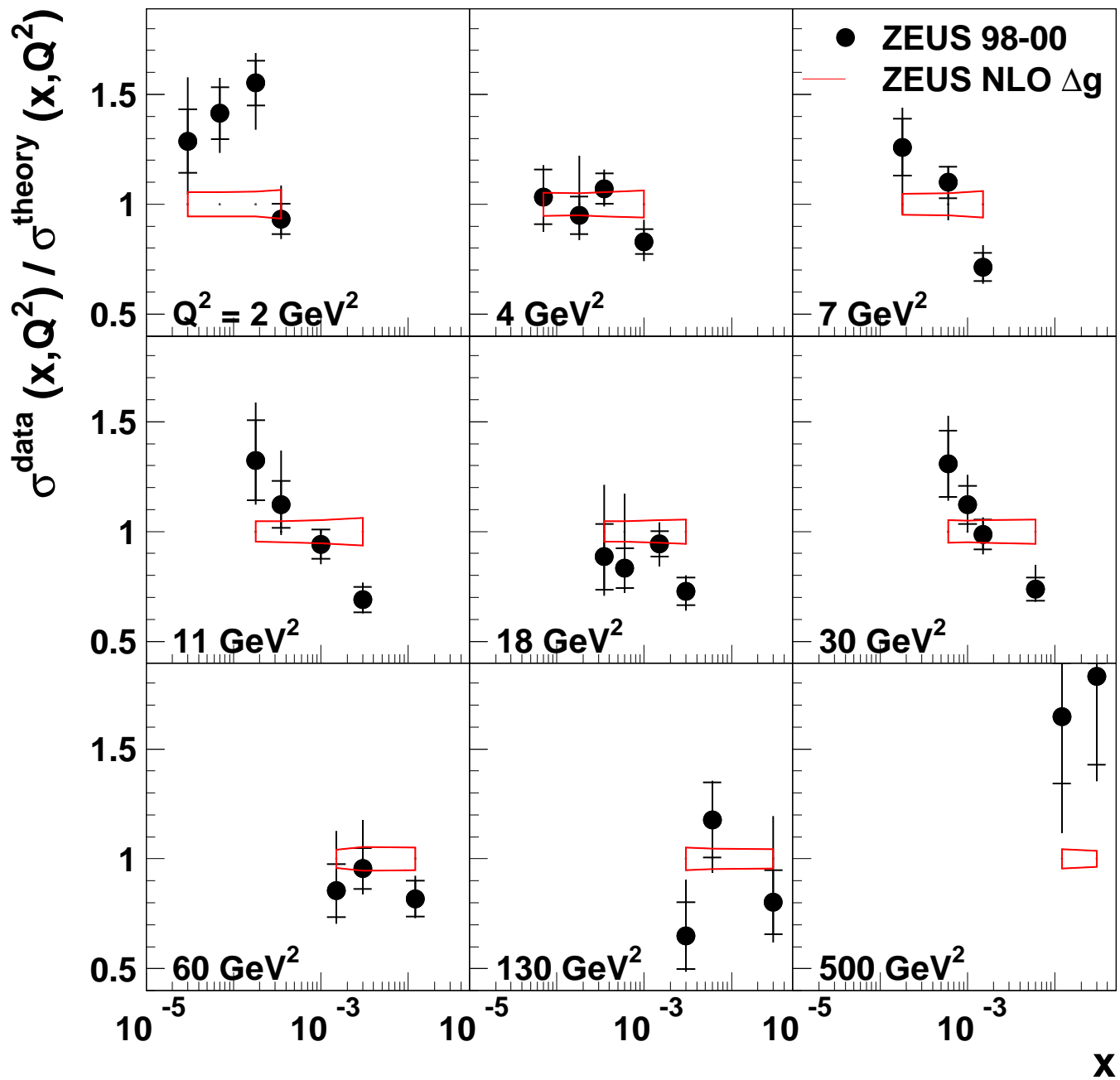
D* production



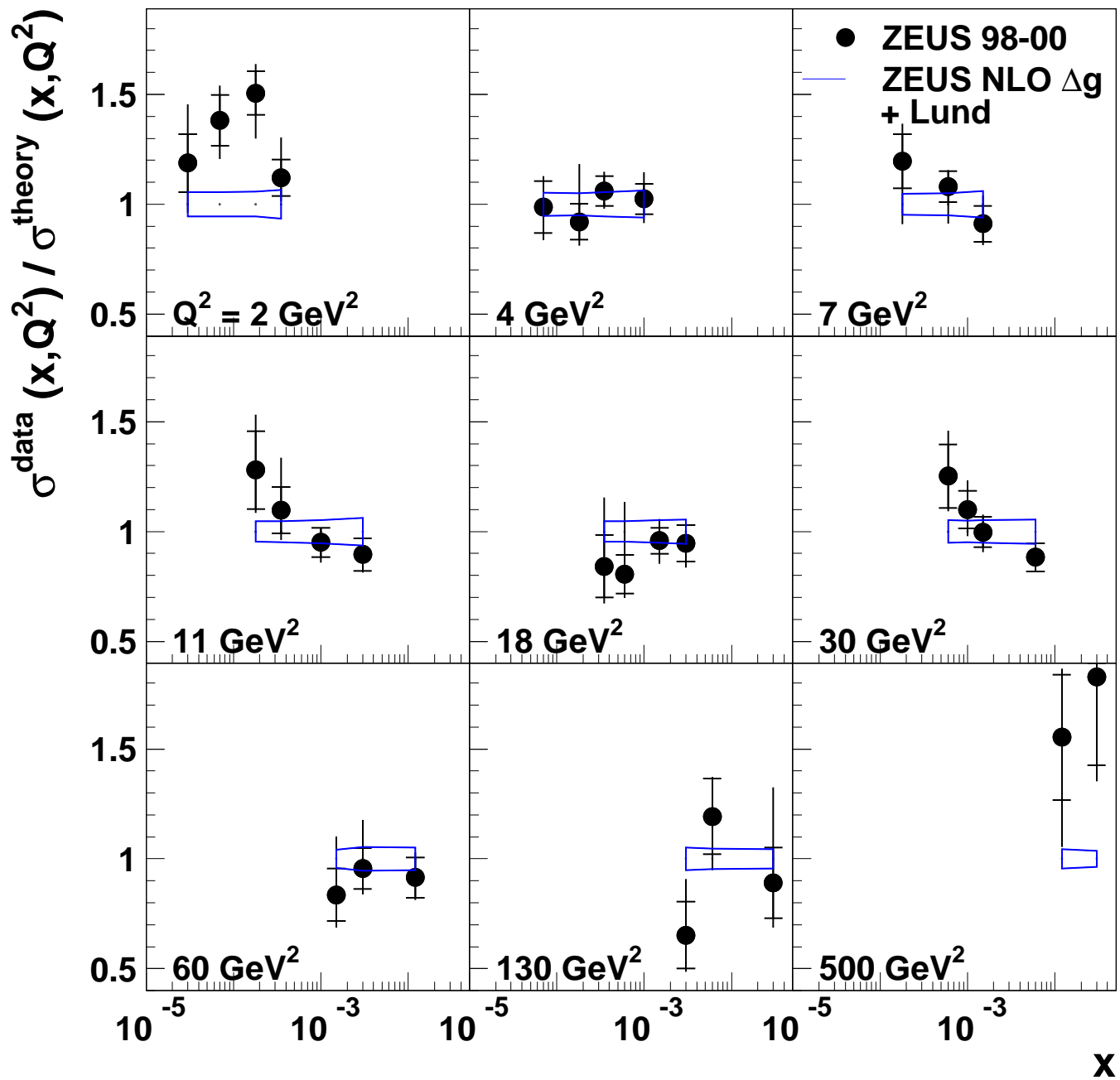
D* production



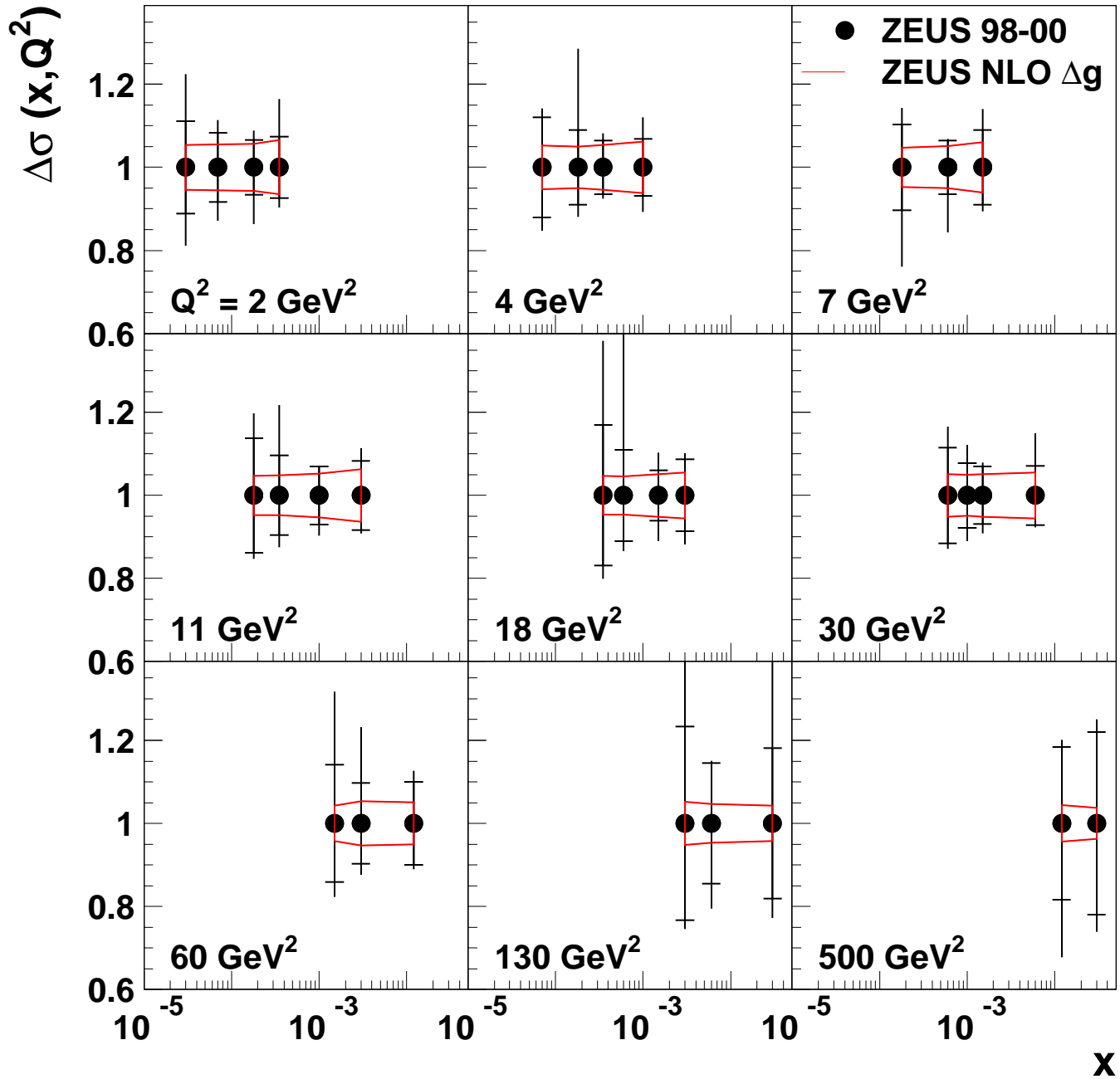
D* production

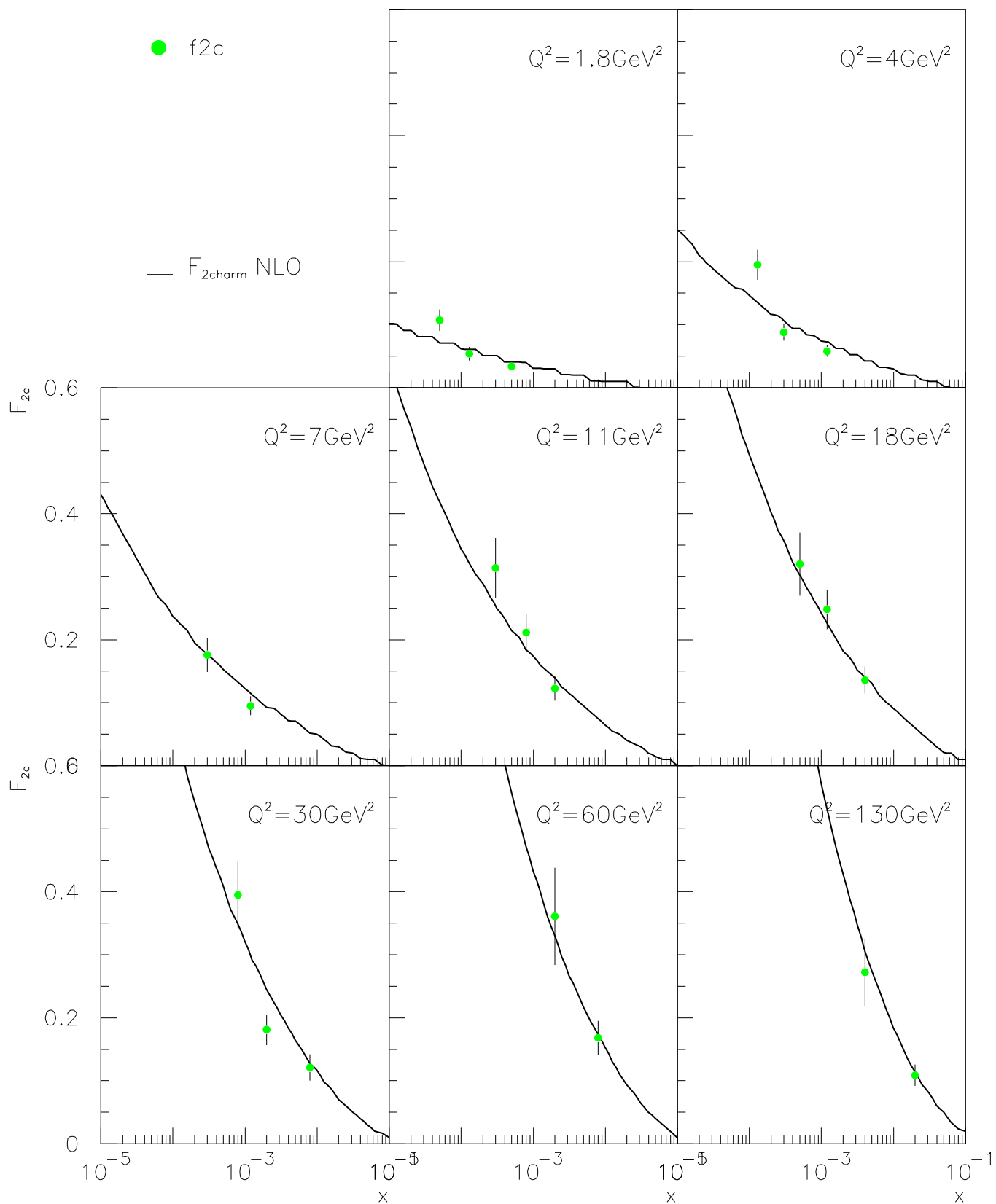


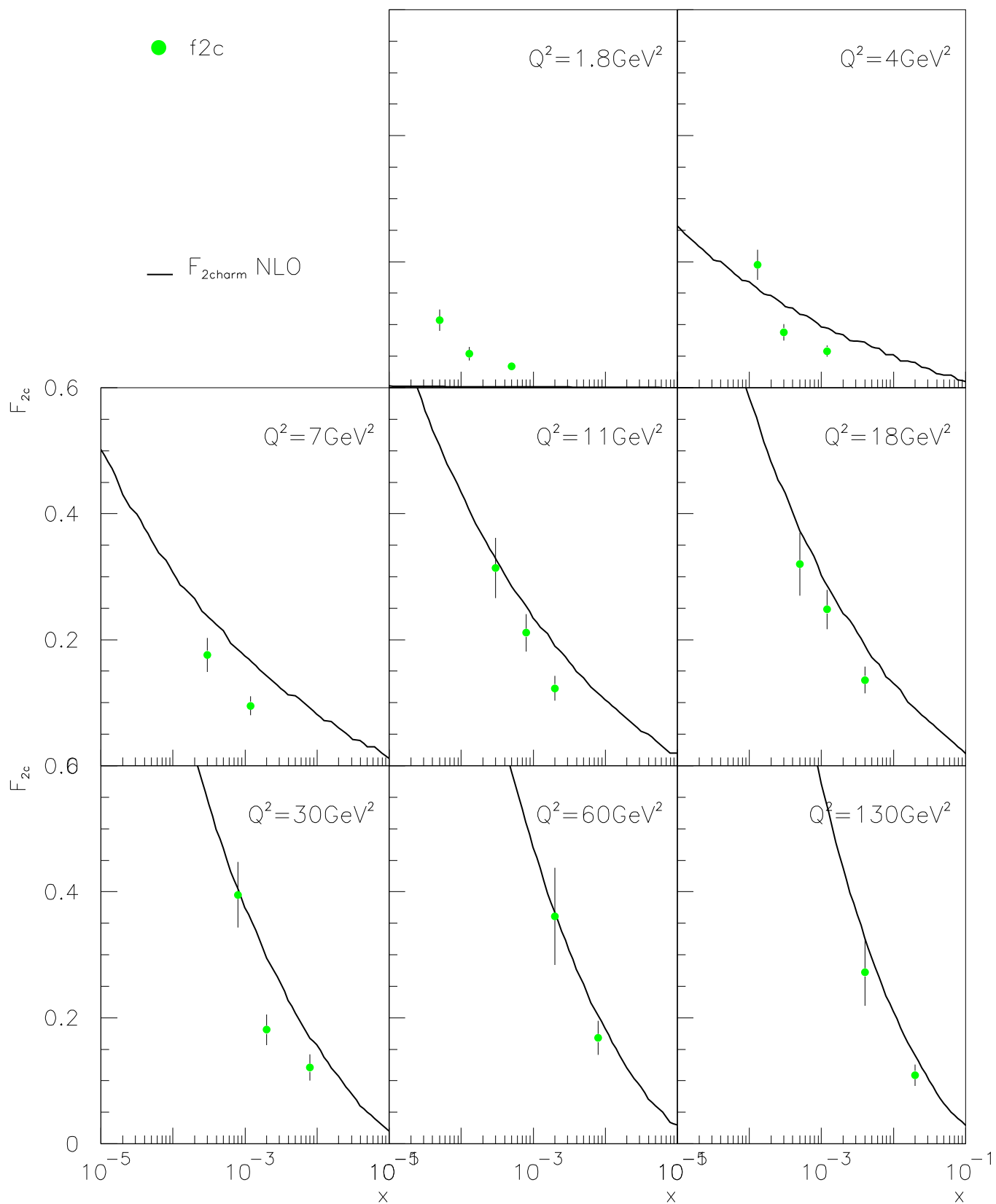
D* production

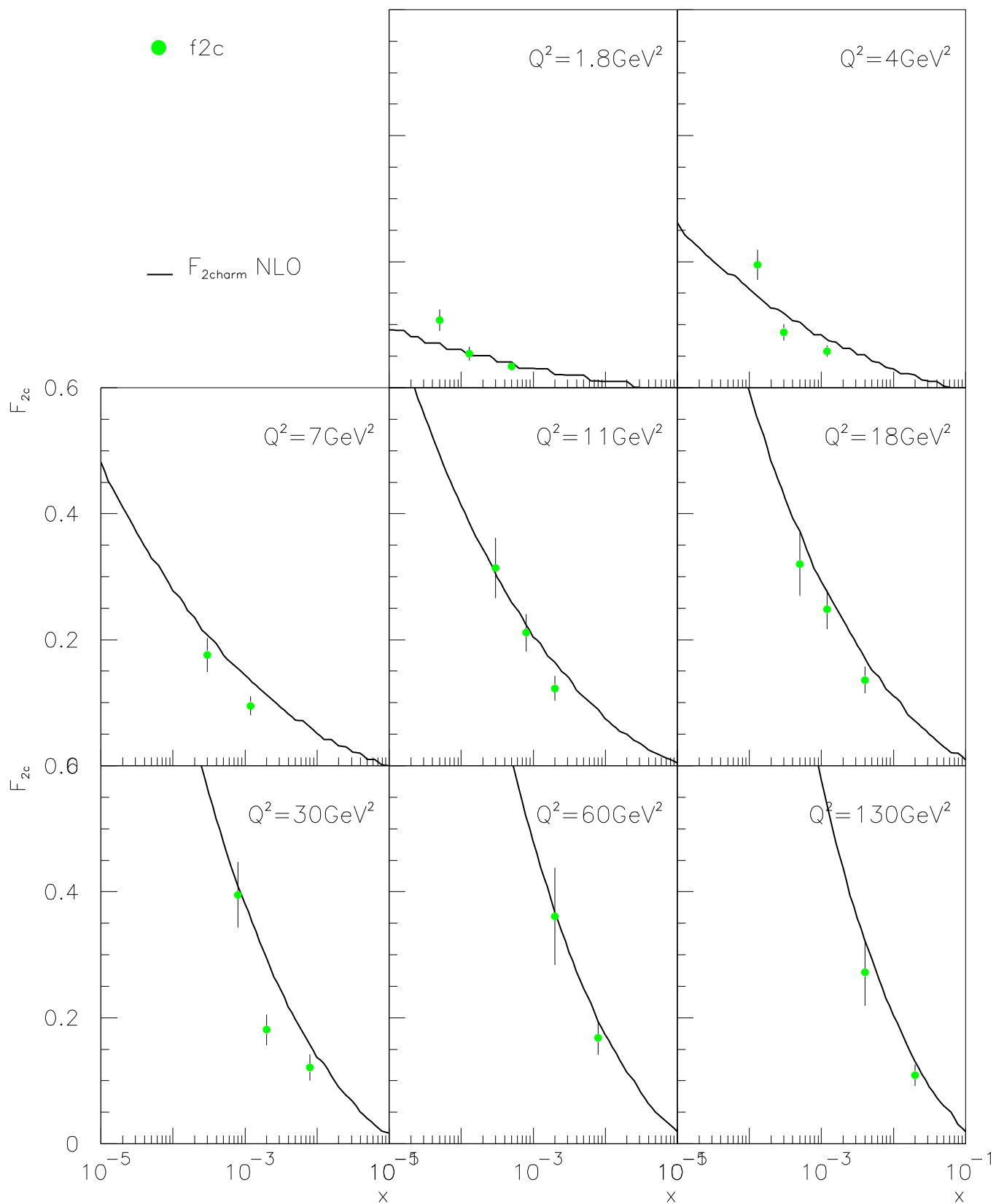


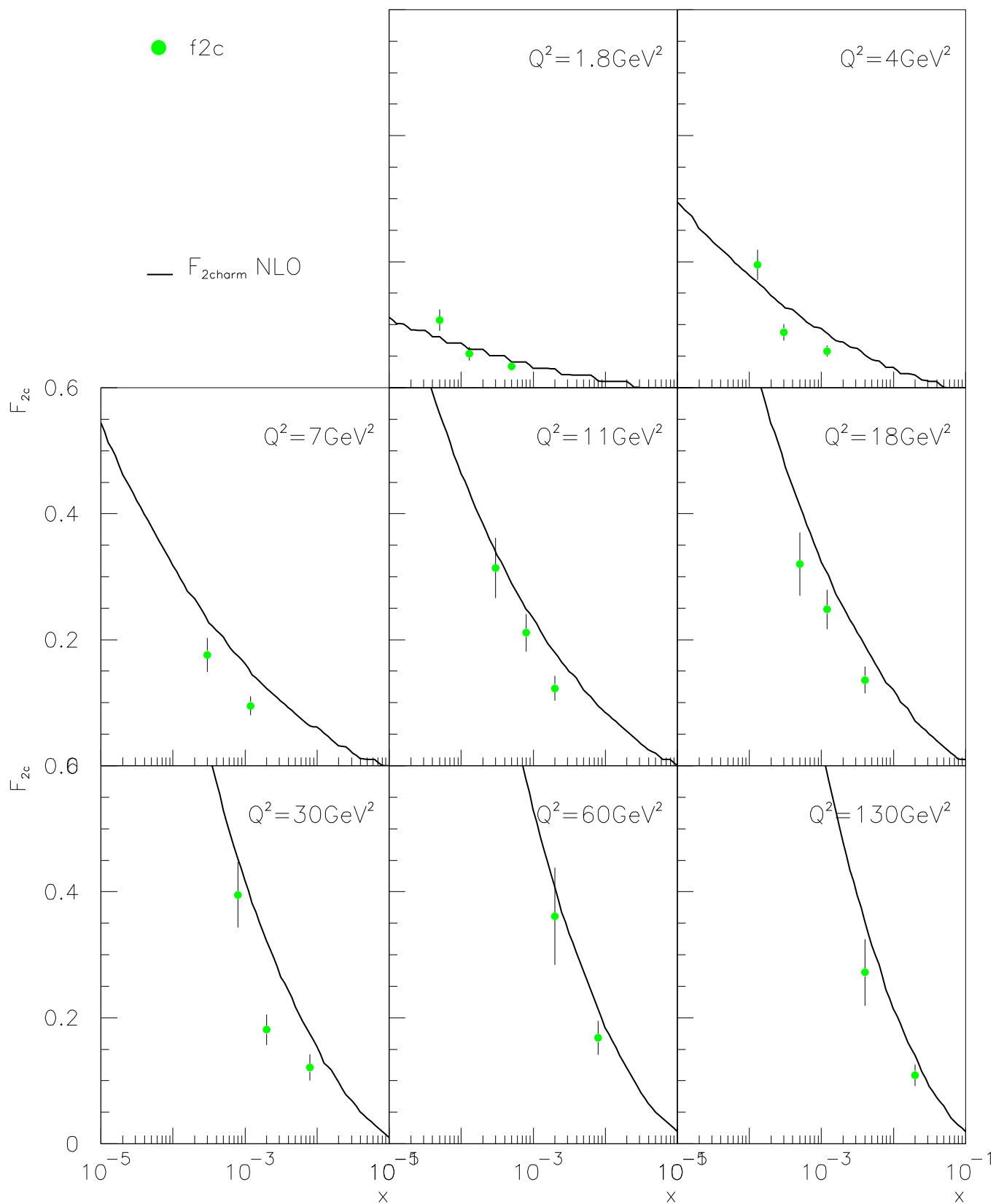
D* production

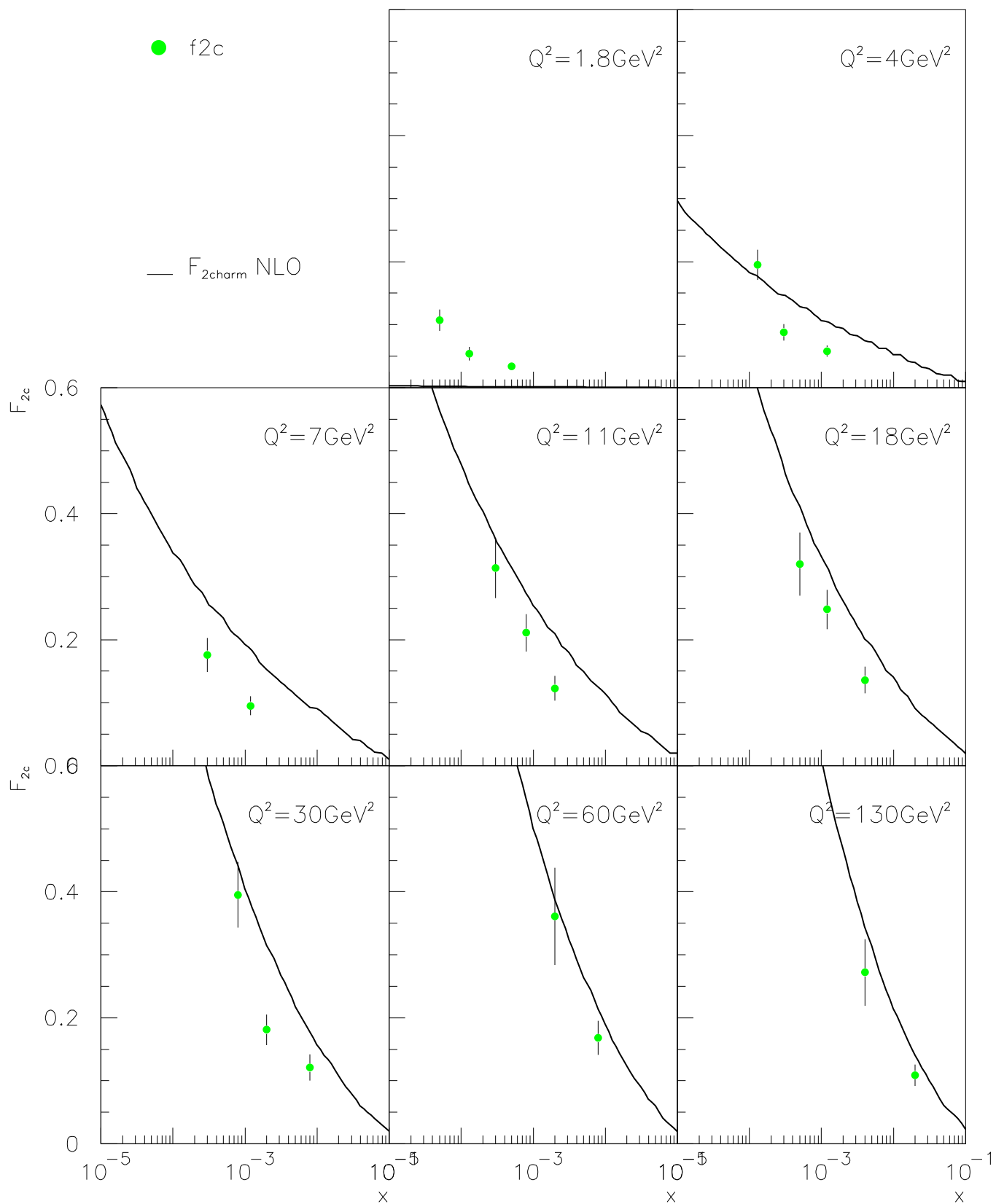


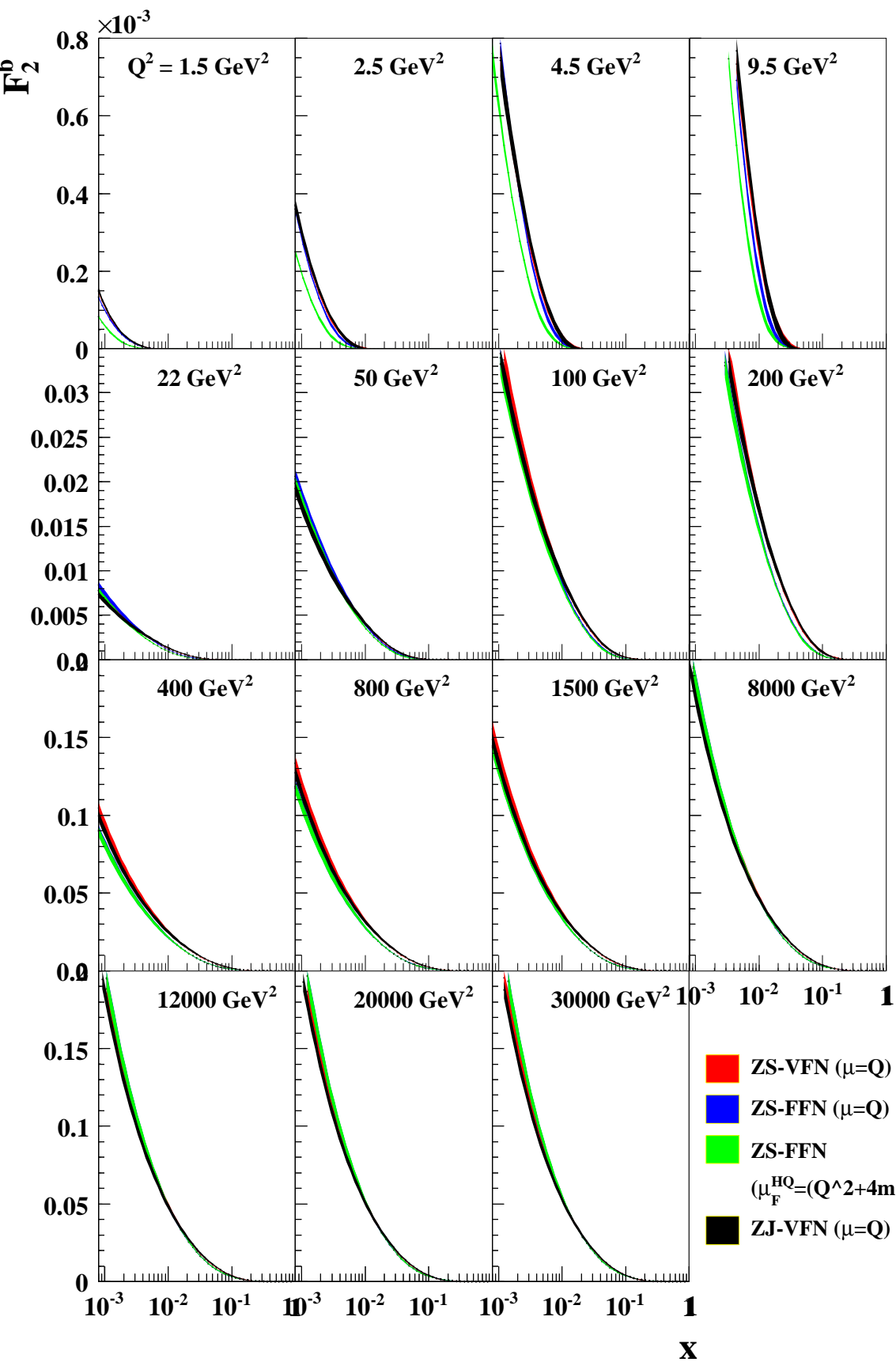


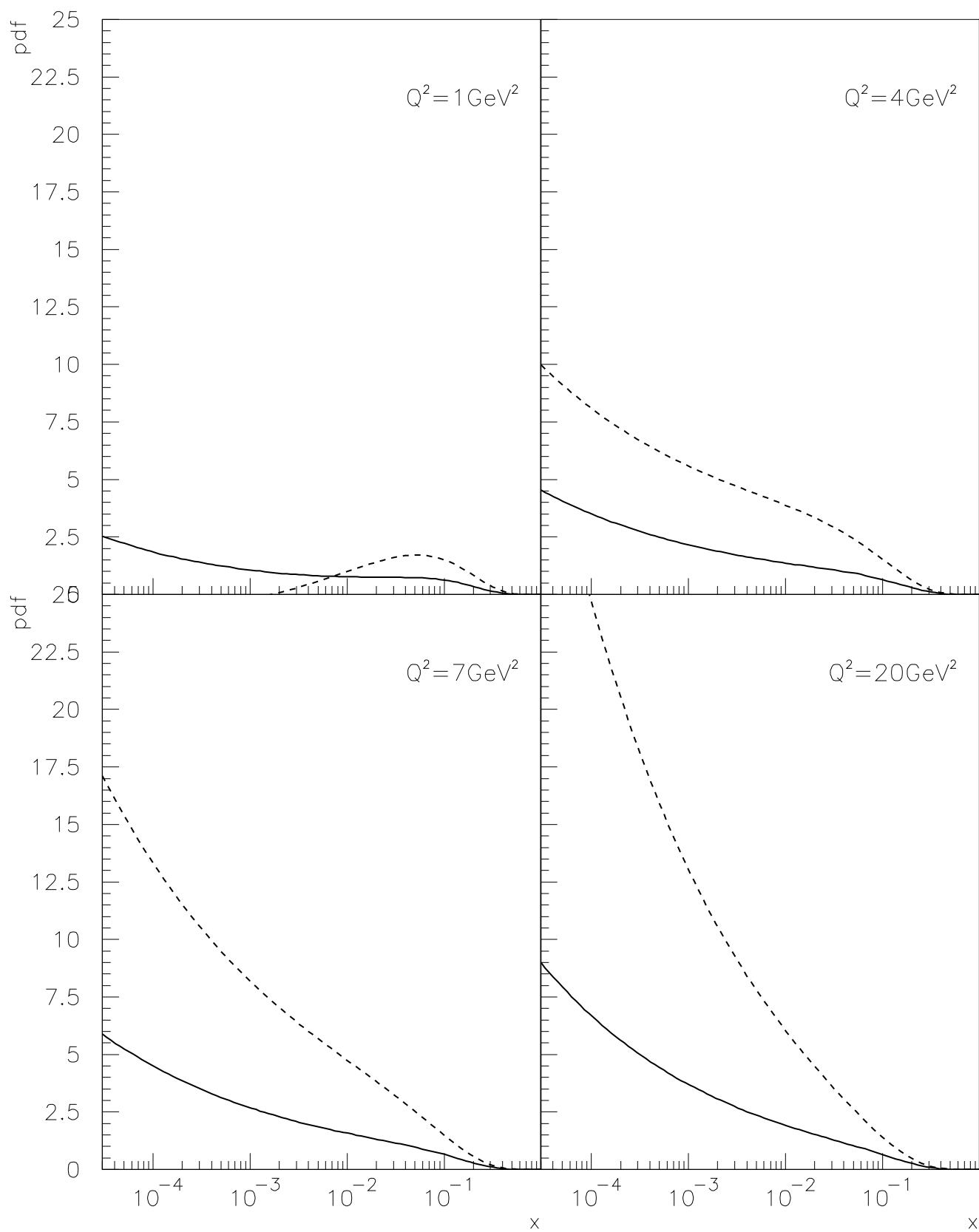


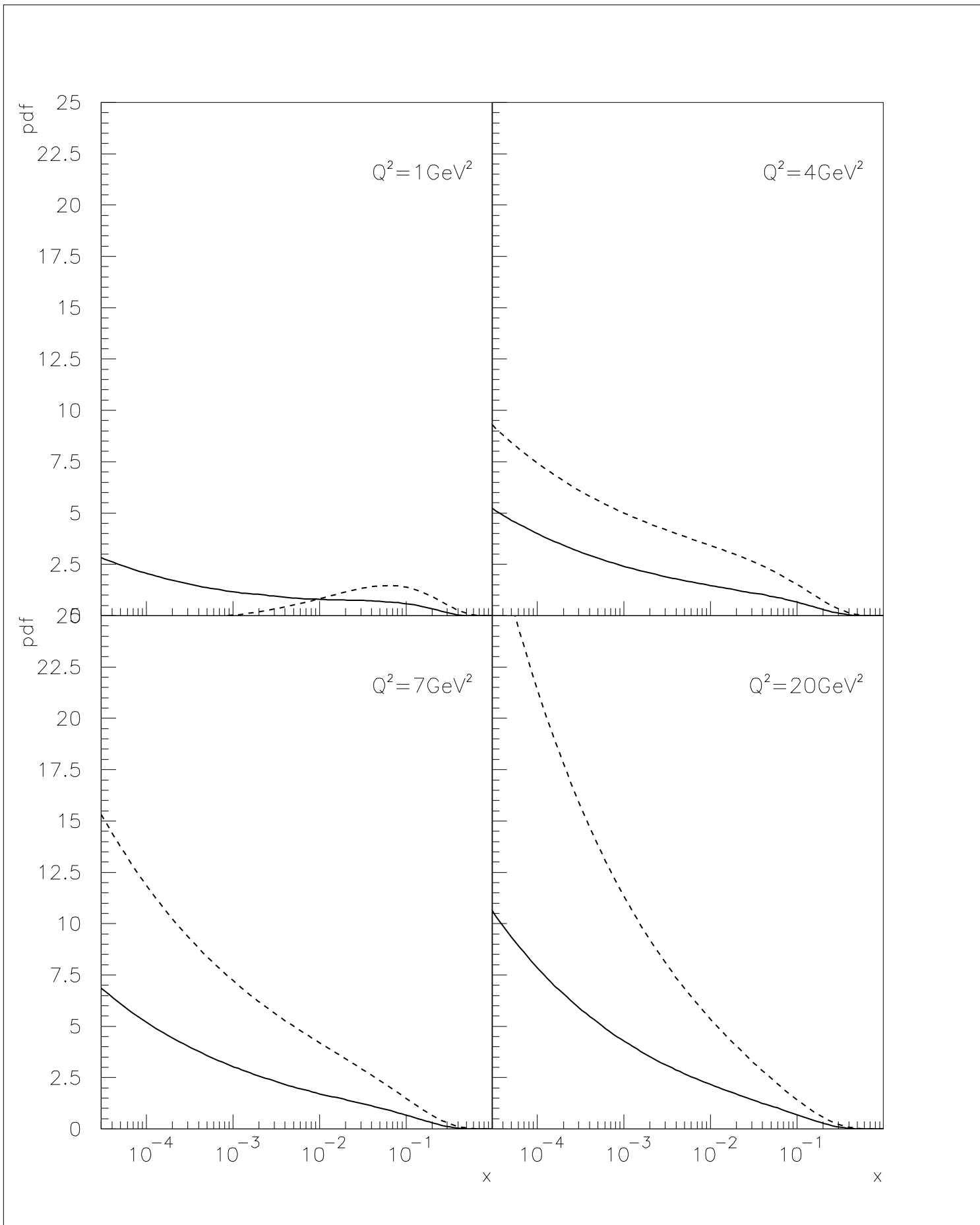


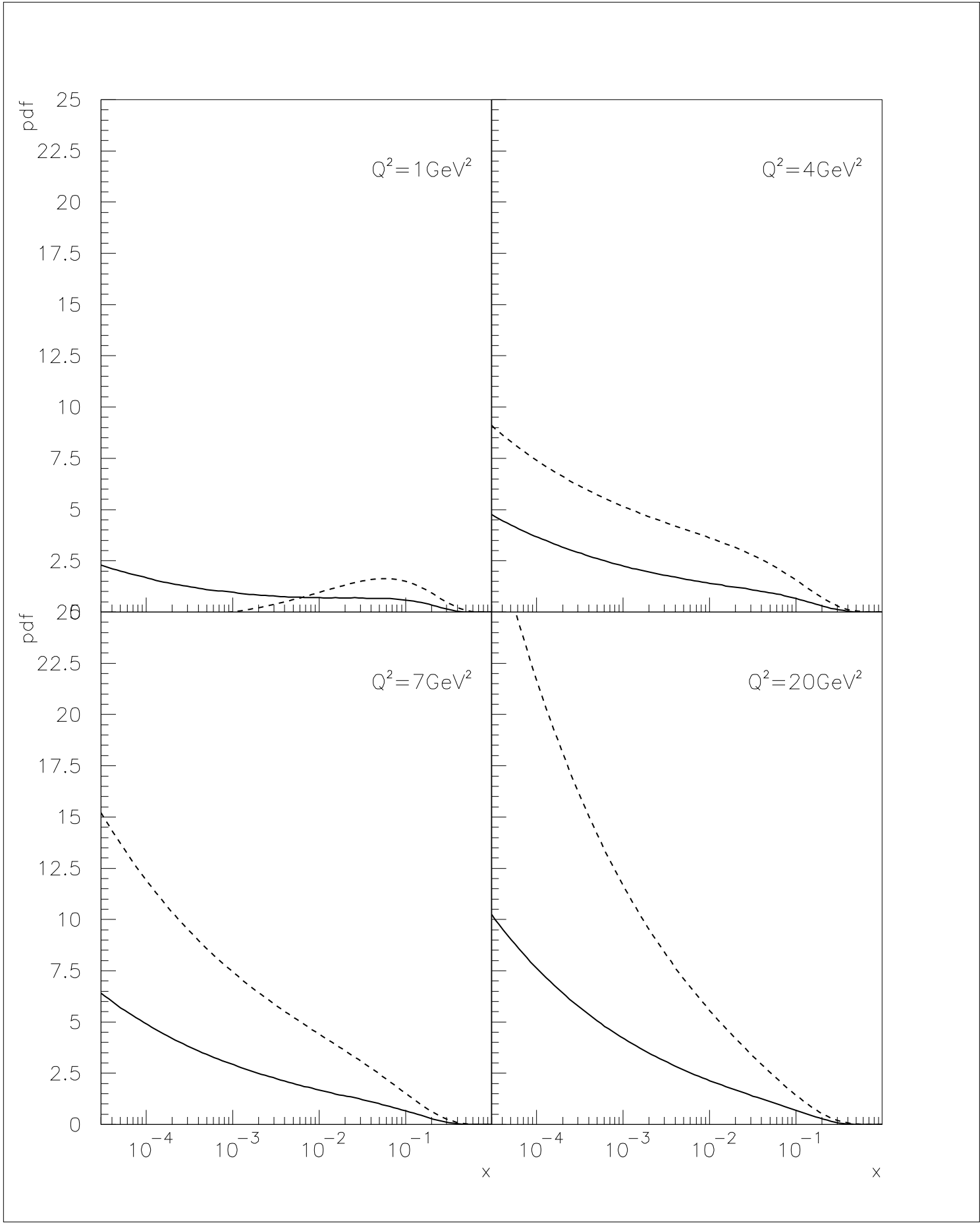












D* production

